Food Hydrocolloids 28 (2012) 82–91

Contents lists available at SciVerse ScienceDirect

Food Hydrocolloids

journal homepage: www.elsevier.com/locate/foodhyd

Formation of zein nanoparticles by electrohydrodynamic atomization: Effect of the main processing variables and suitability for encapsulating the food coloring and active ingredient curcumin

J. Gomez-Estaca, M.P. Balaguer, R. Gavara, P. Hernandez-Munoz*

Instituto de Agroquímica y Tecnología de Alimentos (IATA-CSIC), Grupo de Envases, Av. Agustín Escardino 7, 46980 Paterna, Valencia, Spain

ARTICLE INFO

Article history:
Received 24 March 2011
Accepted 29 November 2011

Keywords:
Electrohydrodynamic atomization
Curcumin
Zein
Encapsulation
Nanoparticles

ABSTRACT

Nanoparticles with a compact spherical structure and a narrow size distribution were prepared from a zein protein polymer by electrohydrodynamic atomization. The effects of key parameters of the process (polymer concentration, flow rate and applied voltage) on the size and morphology of the particles was studied. Zein nanoparticles could be obtained from zein concentrations ranging from 2.5% to 15% (w/w). The sizes of these particles, ranging from 175 to 900 nm, increased with increasing polymer concentration. Compact nanostructures were obtained for 2.5% and 5% zein solutions whereas 10% and 15% solutions yielded collapsed and shrunken particles. Flow rate also exerted an effect, the lower the flow rate the smaller the nanoparticles. The morphology of the nanoparticles did not change after incorporating curcumin in proportions ranging from 1:500 to 1:10 (curcumin:zein), and the encapsulation efficiency was around 85–90%. Fluorescence microscopy images showed that the nanostuctures obtained took the form of matrix systems with the curcumin homogeneously distributed in the zein matrix. The curcumin remained in the amorphous state in the nanoparticle, as revealed by X-Ray diffractometry, evidencing intimate contact with the polymer. After three months of storage at 23 °C and 43% relative humidity in the dark, neither the size or the morphology of the nanoparticles had undergone significant changes, nor had the curcumin content altered. Thanks to encapsulation, the curcumin presented good dispersion in an aqueous food matrix: semi-skimmed milk.

1. Introduction

Curcumin [1,7-bis(4-hydroxy-3-methoxyphenyl)-1,6-heptadiene-3,5-dione] is a polyphenol found in the rhizomes of the plant *Curcuma longa*. *C. longa* extracts contain three different diarylheptanoids: curcumin, demethoxycurcumin, and bisdemethoxycurcumin (Jayaprakasha, Rao, & Sakariah, 2002). Commercially available curcumin generally consists of a mixture of these three naturally occurring curcuminoids, with curcumin as the main constituent (Ahsan, Parveen, Khan, & Hadi, 1999). Traditionally, curcumin has been employed as a natural food dye which impairs an attractive bright yellow–orange color. Furthermore, curcumin has been shown to possess antioxidant (Jayaprakasha, Rao, & Sakariah, 2006; Sreejayan & Rao, 1997), anti-inflammatory (Ammon & Wahl, 1991; Jurenka, 2009), antimicrobial (Kim, Choi, & Lee, 2003; Wang, Lu, Wu, & Lv, 2009), anticancer (Villegas, Sanchez-Fidalgo, & de la Lastra, 2008; Yoysungnoen, Wirachwong, Changtam, Suksamram, & Patumraj, 2008) and wound-healing (Biswas & Mukherjee, 2003) properties. Current consumer demands for more natural foods with fewer synthetic additives, together with this wide range of biological activities, have made curcumin a focus of interest for both researchers and the food industry. However, certain problems limit the use of curcumin in foods: its low water solubility (Wang, Lu, Lv, & Bie, 2009), which may limit its dispersion in food matrices; its low bioavailability, which negatively affects its biological efficacy (Shaikh, Ankola, Beniwal, Singh, & Kumar, 2009); and its rapid degradation under neutral or alkaline pH conditions or when exposed to light (Tonnesen, 2002).

Encapsulation involves immobilizing a particular compound in a material that coats it or in which it is dispersed. Encapsulation processes are widely used in various industrial sectors, such as pharmaceuticals, agrochemicals and foodstuffs. Encapsulation can improve the organoleptic characteristics of a product, masking undesirable flavors, odors and colors; facilitate the handling and dosing of certain ingredients and additives which pose problems of volatility, stickiness or low solubility in water; or release the active compound at controlled rates or under specific conditions. Encapsulation can also protect the molecule from degradation or loss of functionality due to the effects of light, oxygen, pH, moisture or interaction with other food matrix components.

* Corresponding author. Tel.: +34 963900022; fax: +34 963636301.
E-mail address: phernan@iata.csic.es (P. Hernandez-Munoz).

0268-005X/$ – see front matter © 2011 Elsevier Ltd. All rights reserved.
doi:10.1016/j.foodhyd.2011.11.013

Attempts have been made to encapsulate curcumin by several methods, including chemical/physico-chemical and physico-mechanical techniques. There are reports of its being incorporated into cyclodextrins (Baglole, Boland, & Wagner, 2005), liposomes (Li, Ahmed, Mehta, & Kurzrock, 2007), microemulsions (Lin, Lin, Chen, Yu, & Lee, 2009), micelles (Yu & Huang, 2010) and super-paramagnetic silica reservoirs (Chin et al., 2009), as well as of the development of micro or nanoparticles by spray-drying (Wang et al., 2009), solvent emulsion–evaporation (Mukerjee & Vishwanatha, 2009; Prajakta et al., 2009; Shaikh et al., 2009), antisolvent precipitation method (Patel, Hu, Tiwari, & Velikov, 2010) or ionotropic pregelation followed by polycationic cross-linking (Das, Kasoju, & Bora, 2010) using coating materials such as zein, gelatine, starch, alginate, chitosan, pluronic or polylactic-co-glycolic acid.

Nowadays, research on nanostructures is receiving much attention because of the unusual properties that materials on the nanometer length scale acquire (Huang, Yu, & Ru, 2010). One of the main benefits of nanotechnology in the active compound encapsulation field derives from the greater specific surface of the particles, which improves their dispersion and even enhances the bioavailability of the encapsulated compounds. For example, there were developed zein–curcumin colloidal nanoparticles by antisolvent precipitation method, achieving good solubilization in an aqueous medium (Patel et al., 2010).

Electrohydrodynamic atomization (EHDA) or electrospray is a well-known method for preparing monodisperse nanoparticles from a multitude of different precursors. EHDA has been used to produce inorganic nanoparticles, drug nanoparticles and polymeric drug delivery nanoparticles and to encapsulate drugs with poor solubility in water. This technique relies on the break-up of a liquid into fine charged droplets under the action of an electric field. Commonly, the electrospray is generated when a liquid is passed through a thin metal tube such as a nozzle, capillary or needle and the liquid meniscus located at the tip of the tube is electrically stressed by applying a potential difference between the tube and the counter electrode. Depending on the strength of the electric field, the flow rate and the properties of the liquid, different spraying modes are achieved. The most effective mode of obtaining a narrow size distribution of small droplets is to work in the cone-jet mode, also known as the stable non-pulsating Taylor cone. In this electrospray mode the pendant drop adopts the shape of a cone and the liquid at the tip of the cone takes the shape of a fine jet (Hartman, Brunner, Camelot, Marijnissen, & Scarlett, 2000).

EHDA presents several advantages compared to other micro- and nanoparticle manufacturing techniques. For instance, EHDA possesses high encapsulation efficiency and does not require a tedious separation process to remove the particles from the solvent, as happens with a great variety of encapsulation techniques. Moreover, EHDA allows particles of different diameters with a narrow size distribution to be obtained with ease. The particle structure can be obtained from matrix systems when working with one electrified jet, while more sophisticated structures such as hollow nanoparticles and core-shell particles are possible when working with coaxial electrified jets.

Zein, the maize prolamin protein, was selected as the encapsulating material. Zein comprises a group of alcohol soluble proteins which present the property of being insoluble in water (Shukla & Cheryan, 2001). The literature contains some works regarding the utilization of zein as a wall material for encapsulating a variety of compounds in the food, pharmaceutical and agricultural fields (Liu, Sun, Wang, Zhang, & Wang, 2005; Onal & Langdon, 2005; Parris, Cooke, & Hicks, 2005; Patel et al., 2010; Zhong & Jin, 2009; Zhong, Jin, Davidson, & Zivanovic, 2009), including antimicrobials (essential oils, lysozyme), drugs (ivermectin, gitoxin), vitamins (riboflavin) and polyphenols (curcumin). In these studies, zein micro- and nanoparticles were produced by methods such as phase separation, spray-drying, coacervation, and antisolvent precipitation. Zein nanostructures in the form of nanofibers, as carriers of antioxidant natural compounds, have also been obtained by electrospinning (Li, Lim, & Kakuda, 2009). However there is no previous report on the study of zein nanoparticle formation using EHDA.

The first objective of the present study was to explore the use of the EHDA technique to obtain zein nanoparticles. For this purpose, the effect of relevant electrospray processing parameters (polymer concentration, applied voltage and flow rate) on the size and shape of the resulting zein structures was studied. The next objective was to incorporate the natural food dye and active compound curcumin into zein nanoparticles developed by EHDA and to study the morphology, some physical properties, and stability during storage of the curcumin-loaded zein nanoparticles. Finally, the effectiveness of the developed curcumin-loaded zein nanoparticles as coloring in a food matrix, semi-skimmed milk, was evaluated.

2. Materials and methods

2.1. Materials

Zein from maize and curcumin from *Curcuma longa* (turmeric) were purchased from Sigma Chemical Co. (St. Louis, MO, USA). Ethanol was acquired from Panreac (Barcelona, Spain).

2.2. Molecular weight profile of zein

The molecular weight of the industrial sample of zein was determined by SDS-PAGE in a vertical electrophoresis unit (Bio-Rad Laboratories, Hercules, CA, USA). The procedure was that of Laemmli (1970) with slight modifications. The sample was denatured by mixing 2 mg of zein with 1 mL of loading buffer (2.5% SDS, 10 mM Tris–HCl, 1 mM EDTA, 6% glycerol, 0.01% bromophenol blue). The sample-buffer mixture was allowed to stand at room temperature for 2 h with occasional shaking and centrifuged at 13,000 g for 10 min. Afterwards, 10 μL of each sample were loaded into each slot in the gel. The stacking gel was 4% acrylamide and the resolving gel was 12% acrylamide. Electrophoresis was carried out at 25 mA/gel over 1.5 h. The gels were stained with coomassie brilliant blue. The molecular weights of the standard protein mixture (Bio-Rad) were 199 kDa (myosin), 116 kDa (β-galactosidase), 97 kDa (bovine serum albumin), 53 kDa (ovalbumin), 37 kDa (carbonic anhydrase), 29 kDa (soybean trypsin inhibitor), 20 kDa (lysozyme) and 7 kDa (aprotinin).

2.3. Preparation and properties of zein solutions

Zein was dissolved in 80% (w/w) aqueous ethanol and stirred for 30 min at room temperature until completely dissolved. Several concentrations of zein in ethanol were prepared, ranging from 1% to 20% (w/w).

The viscosity of the polymer solutions was determined with a Thermo Haake Rheostress 1 rotary rheometer (Karlsruhe, Germany) using 60 mm plate–plate geometry with a gap of 0.5 mm. Flow curves were obtained by shearing up from 0.1 to 100 s^{-1} and shear stress was recorded.

2.4. Nanoparticle production

The experimental set-up used to carry out the electrohydrodynamic atomization of the hydroalcohlic solution consisting of zein polymer or zein polymer and curcumin was supplied by YFLOW Ltd (Málaga, Spain). It consists of a stainless steel needle charged by a high voltage power supply with a range of 0–30 kV. The collector

plate was fixed at a working distance of 7 cm below the needle tip and connected to the grounded counter electrode of the power supply. A 5 mL plastic syringe was filled with the solution and a syringe pump was used to control the flow rate at which the solution was dispensed. The syringe outlet was connected to the needle through a Teflon® pipe. A video camera connected to a monitor was used to monitor the cone-jet mode. The electrospray droplets were dried during the fly time, on the way to the surface of the collector plate, which was previously covered with aluminum foil. The relative humidity and temperature of the chamber were set at 30% and 25 °C, respectively.

The effect on the shape and size of the zein structures of the main electrospray variables, namely the polymer concentration in the aqueous ethanol, the flow rate and the applied voltage, was investigated to determine the optimal conditions for obtaining homogeneous nanoparticles.

2.5. Nanoparticle morphology

The particle morphology was studied by scanning electron microscopy using a HITACHI S-4100 unit equipped with a BSE AUTRATA detector and an EMIP 3.0 image capture system (HITACHI, Madrid, Spain). The samples were collected on an aluminum sample holder, which was placed on the surface of the collector plate. The samples were kept at 0% RH, in the dark, and treated with gold–palladium immediately prior to analysis. Images were captured at 10 kV, at a distance of 5 cm, with 5000× and 20,000× magnification.

2.6. Curcumin-loaded zein nanoparticles and encapsulation efficiency (EE)

Once the best processing conditions to obtain zein nanoparticles had been established, curcumin-loaded zein nanoparticles were prepared. For this purpose, curcumin was added to the zein solution at different weight ratios ranging from 1:500 to 1:10 (curcumin:zein) and the solutions were electrosprayed. Samples were collected on an aluminum foil placed over the collection plate and stored at 0% RH, in the dark, until they were analyzed.

The curcumin loaded in the nanoparticles was measured by dissolving the nanoparticles in 80% (w/w) aqueous ethanol and measuring the absorbance of curcumin at 428 nm using a UV–Vis spectrophotometer. In previous experiments it had been checked that the presence of zein in the solution did not interfere with the maximum absorbance peak of curcumin. The concentration of curcumin in the sample was calculated from the previously prepared standard calibration curve for curcumin in 80% (w/w) ethanol. The EE of curcumin was obtained as the mass ratio between the curcumin determined in the nanoparticles and that used in the preparation of the nanoparticles.

2.7. Fluorescence microscopy

The distribution of curcumin in the zein nanoparticles was investigated by fluorescence microscopy because curcumin presents autofluorescence. The fluorescence microscope used was a Nikon Eclipse 90i equipped with a Digital Sight DS-5Mc refrigerated digital camera. The samples were collected on a glass sample holder and observed under a blue filter (excitation at 340–380 nm, emission at 345–485), green filter (excitation at 465–495 nm, emission at 515–555 nm) and red filter (excitation at 540, emission at 605–655) and without attenuation filters. Photographs were taken at 1000×.

2.8. Solid state characterization

X-ray powder diffractometry was carried out to investigate the nature of the curcumin loaded in the zein nanoparticles. The XRD patterns of commercial curcumin, curcumin-loaded zein nanoparticles and unloaded zein nanoparticles were recorded using a Bruker AXS D500 spectrometer with a Bragg–Brentano geometry at a wavelength of 1.5406 (corresponding to the $Cu_{k\alpha}$ peak). Powder X-ray diffractograms were recorded in a diffraction angle (2θ) range of 2°–40° using a step size of 0.03° and an exposure time of 8 s.

2.9. Optical properties

The color of the nanoparticles was determined with a Konica Minolta CM-35000d spectrophotometer set to D65 illuminant/10° observer. The CIELAB color space was used to determine the parameters: L^* [black (0) to white (100)], a^* [greenness (−) to redness (+)] and b^* [blueness (−) to yellowness (+)]. The color was expressed using the polar coordinates $L^*C^*h^\circ$ where L^* is the same as above, C^* is the chroma or saturation index ($C^* = (a^{*2} + b^{*2})^{1/2}$) and h° is the hue ($h^\circ = \text{arctg}(b^*/a^*)$). The total color difference (ΔE) was also calculated according to the equation: $\Delta E = [(\Delta L^*)^2 + (\Delta a^*)^2 + (\Delta b^*)^2]^{1/2}$. Samples were measured in triplicate and ten measurements were taken of each sample.

2.10. Curcumin-loaded zein nanoparticle stability studies

Stability studies were carried out for 1:10 curcumin:zein nanoparticles. The nanoparticles were stored in the dark in desiccators at 23 °C and 43% relative humidity over a period of three months. Curcumin-loaded zein nanoparticles were monitored for changes in particle size and shape, the nature of the curcumin solid state (crystal/amorphous ratio) and the curcumin content of the nanoparticle. The sampling time points were at 7, 15, 30, 60 and 90 days of storage.

2.11. Coloring capacity of curcumin-loaded zein nanoparticles in an aqueous food matrix

Semi-skimmed milk (commercially acquired, subjected to conventional industrial homogenization and UHT treatments) was selected as an aqueous food matrix to assay the food coloring capacity of the curcumin incorporated into the zein nanoparticles. For this purpose, zein nanoparticles containing 10% (w/w) curcumin (1:10 curcumin:zein proportion) were incorporated into the food matrix to achieve curcumin concentrations of 0.05, 0.1 and 0.15 g/100 mL of milk and were stirred for 15 min. The milk color was determined, as described above, by placing 5 mL of milk in a glass sample holder, 40 mm in diameter. For the purposes of comparison, a sample with 0.1 g commercial curcumin/100 mL of milk and a blank consisting of 100 mL of milk without additions were analyzed. The color of the samples was evaluated at day 0 and after seven days of refrigerated storage at 4 °C in dark conditions.

2.12. Statistical analysis

Statistical tests were performed using the SPSS® computer program (SPSS Statistical Software, Inc., Chicago, IL, USA). One-way analysis of variance was carried out. Differences between pairs of means were compared using a Tukey test. The level of significance was set at $p \leq 0.05$.

3. Results and discussion

3.1. Nanoparticle production

The main variables that affect the electrospray process include the properties of the polymer in solution (concentration, molecular weight, viscosity, surface tension, conductivity of the solvent) and the processing conditions (flow rate, applied voltage and distance

between the tip and the collector plate). In this study, the effect of zein concentration, flow rate and applied voltage on the size and morphology of the zein structures were explored.

3.1.1. Zein molecular weight

The molecular weight profile of a polymer is an important factor that must be known before undertaking an electrospray process. Low molecular weight polymers lead to the formation of debris and a higher concentration of polymer in the solution is required for the formation of particles, whereas high molecular weight polymers present a great number of entanglements, allowing the formation of particles with a low concentration of polymer. Zein consists basically of two subunits: α-zein, which is soluble in 95% ethanol and is made up of two bands of around 24 and 22 kDa respectively, and β-zein, which is soluble in 60% ethanol and is composed of α-zein aggregates cross-linked by disulfide bonds (Shukla & Cheryan, 2001). However, β-zein is somewhat unstable and tends to coagulate and precipitate, so it is not commonly present in commercial zein preparations (Shukla & Cheryan, 2001). The molecular weight profile of the commercial zein employed in the present study under both disulfide reducing and non-reducing conditions is shown in Fig. 1. There are two bands close together in the 19 to 29 kDa molecular weight range, which can be attributed to the subunits of α-zein previously reported at 22 and 24 kDa (Shukla & Cheryan, 2001). Furthermore, a diffuse band can be seen at around 50 kDa, which may be attributed to covalently linked α-zein dimmers (Landry & Guyon, 1984) as this band disappears when the protein is subjected to disulfide bond reduction conditions. The other narrow bands of high molecular weight at the top of the gel may be attributed to residual β-zein. This shows that high molecular weight aggregates that would have raised the average molecular weight were absent, and it was concluded that the zein employed in the present work has an average molecular weight of around 25–30 kDa, so it can be considered as a low molecular weight polymer.

3.1.2. Zein concentration

The effect of polymer concentration on the morphology of the resulting zein structures was studied for concentrations of polymer in aqueous ethanol ranging from 1% to 20% (w/w). In order to study the effect of the zein concentration in the formation of structures, the flow rate was maintained at 0.15 mL/h and the voltage applied was fixed at 14 kV. With these parameters it was possible to work in the cone-jet mode throughout the range of zein concentrations tested.

Previously, the rheological behavior of zein solutions had been studied and data from the ascending flow curve fitted well to the Ostwald de Waele model, indicating that the aqueous ethanol solutions of zein showed Newtonian behavior under the conditions tested in this study. Fig. 2 shows the effect of zein concentration on the viscosity of the solution. As can be observed, the viscosity increased with the concentration of zein in the solution. Fig. 3 shows the morphology of the zein structures obtained with increasing concentrations of zein. As can be observed, at 1% (Fig. 3A) of zein the polymer concentration in the solution was too low for particle formation. At this concentration, there were not enough intermolecular entanglements among polypeptide chains of this low molecular weight polymer to allow the chains to aggregate into spheres after solvent evaporation. Instead, it can be seen that a discontinuous film generated by droplets carrying a low concentration of polymer was formed. When the concentration of zein was increased to 2.5% the formation of compact particles could be observed (Fig. 3B). These were round in shape, with a relatively smooth surface, and between 175 and 250 nm in diameter, showing low size dispersion. Thus, increasing the concentration of polymer in the droplet promotes the entanglement of polymer chains, which impedes droplet fission and leads to the formation of particles. Compact particles have been associated with small droplet size and a low concentration of solutes (Raula, Eerikainen, & Kauppinen, 2004). In the present study, small compact particles could not be achieved for zein concentrations of 1%, which can be related to the low molecular weight of zein compared to other polymers.

When the concentration of zein was increased to 5% (Fig. 3C) the particles maintained their morphology, showing a round shape and compact structure, and the size increased to between 200 and 350 nm. The increase in particle size with higher polymer concentration has been reported for other polymers also, such as polycaprolactone (Xie, Lim, Phua, Hua, & Wang, 2006), Eudragit (Raula et al., 2004) and an elastin-like polypeptide (Wu, MacKay, McDaniel, Chilkoti, & Clark, 2009), and could be related to the greater mass of the polymer in the droplets generated during the electrospray process and to the viscosity of the solution. Viscosity plays a significant role during the break-up and atomization of the liquid jet, and thus influences the droplet size (Tang & Gomez, 1996).

A further increase in polymer concentration to 10% (Fig. 3D) not only gave rise to an increase in the particle size but also to a change in its morphology. The size of the particles was between 450 and 650 nm and they tended to collapse and shrink. This change in morphology could be related to an increase in droplet size along

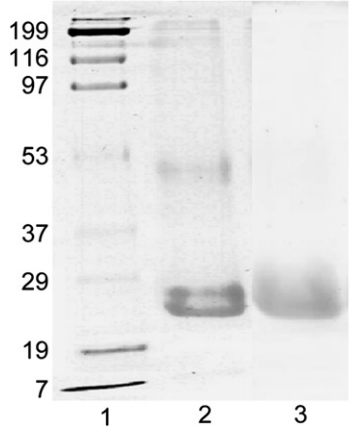

Fig. 1. Electrophoretic patterns of commercial zein under disulphide bond non-reducing (lane 2) and reducing (lane 3) conditions. Lane 1 corresponds to the molecular weight marker (kDa).

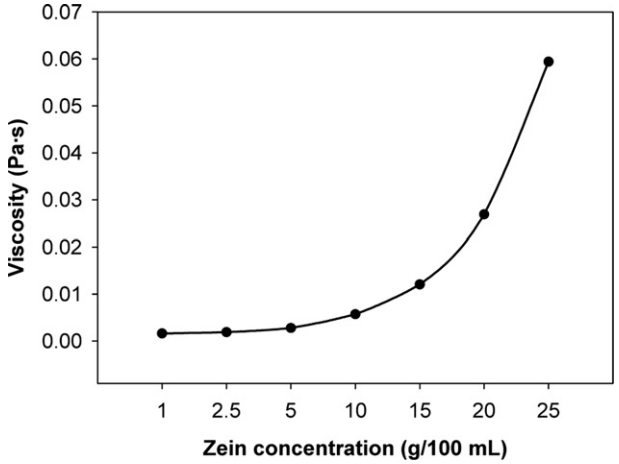

Fig. 2. Viscosity of the polymer solution as a function of zein concentration.

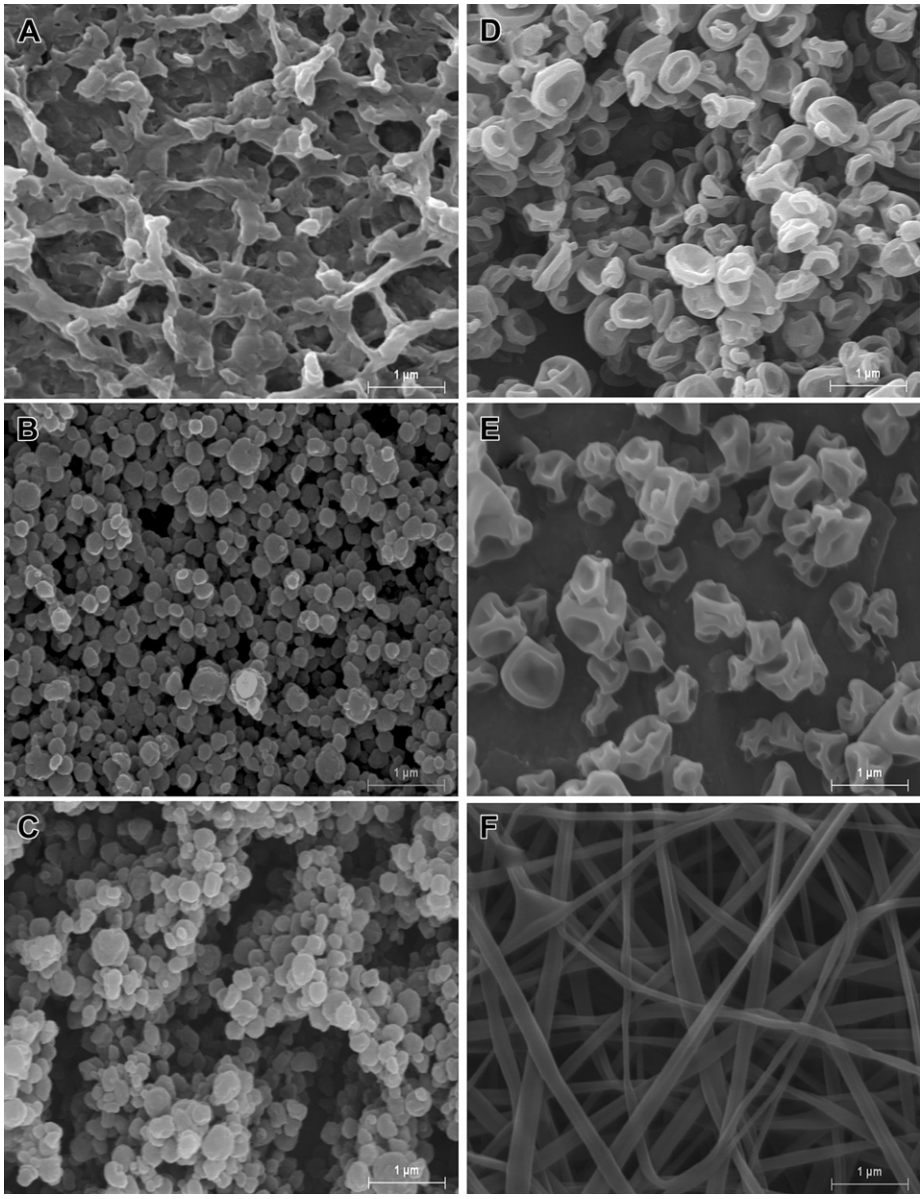

Fig. 3. SEM images showing the effect of zein concentration on the size and shape of nanostructures obtained at a constant flow rate (0.15 mL/h), needle-to-tip distance (7 cm) and voltage (14 kV). A: 1%; B: 2.5%; C: 5%; D: 10%; E: 15%; F: 20%.

with a rapid evaporation of the solvent, creating a polymer concentration gradient along the droplet and the formation of a semi-solid skin of polymer at the surface. The shell layer thus created impeded the diffusion of the solidified polymer to the center of the droplet, inhibiting the formation of compact particles; after drying the shell collapsed and shrunken particles were obtained. However they were not seen to fragment. Li et al. (2009), who studied the formation of zein nanofibers, also obtained shrunken nanoparticles when they used 10% zein solutions under conditions very close to those employed in the present work. Raula et al. (2004) studied the effect of the solvent on the formation of Eudragit particles and obtained different morphologies comprising compact, hollow collapsed, and shriveled structures. As can be observed in Fig. 3E, a further increase in the concentration of zein in the solution to 15% produced particles with similar morphologies and increased particle size: between 450 and 900 nm. Also, the greater particle size with higher zein concentration was observed to be accompanied by greater particle-size dispersion. A zein concentration of 20% (Fig. 3F) gave rise to the transition from particles to fibers, a finding which was in accordance with the work by (Li et al., 2009). As can be observed in Fig. 2, the viscosity of the zein solution increased considerably when the concentration was raised from 15% to 20%. If the viscosity is high enough, a stable elongated jet can be obtained. An increase in the viscosity of the solution promotes a high cohesion and entanglement between polymer chains which prevents the liquid from breaking up into droplets, so a transition from electrospray to electrospinning occurs. In the electrospinning process, the entangled polymer network is stretched and as the jet extends and travels to the ground collector it dries and hardens, resulting in the formation of electrospun fibers. In this study, the transition of zein solutions from electrospray to electrospinning greatly depended on the viscosity of the solution. Uniform fibers without beads were formed for viscosities $\geq$0.027 Pa s, whereas for viscosities between 0.002 Pa s and 0.012 Pa s the zein solution broke into droplets, giving rise to the formation of particles. In this respect, the formation of nanofibers from zein and other proteins is another area of increasing interest for different purposes, including encapsulation (Dror et al., 2008; Li et al., 2009; Woerdeman et al., 2005).

3.1.3. Flow rate

The flow rate is an important parameter in the EHDA process, affecting the size of the particles. Working in the cone-jet mode, it has been described a scaling law which permits prediction of the relationship between several process parameters and the droplet diameter (Hartman, Brunner, Camelot, Marijnissen, & Scarlett, 1999; Hartman et al., 2000). According to this scaling law, the droplet diameter will increase with the liquid flow rate, and the size of the resulting particles is expected to increase. The effect of the flow rate on the diameter of polymeric nanoparticles has been observed by several authors using different polymers (Hong, Li, Yin, Li, & Zou, 2008; Meng, Jiang, Sun, Yin, & Li, 2009; Wu et al., 2009; Xie, Lim, et al., 2006).

In the present study, the effect of the flow rate on the size of the nanoparticles was evaluated with the voltage fixed at 14 kV and the zein concentration at 2.5%; under these conditions it was possible to work in the stable cone-jet mode for flow rates of 0.05, 0.10 and 0.15 mL/h. As can be observed in Fig. 4, the size of the particles decreased with the zein solution flow rate: the nanoparticle diameters were observed to lie between 80 nm and 130 nm for the 0.05 mL/h flow rate, and in the 130–175 nm range when the flow rate was increased to 0.10 mL/h. Fig. 4 also shows that the very fine particles obtained at low flow rates tend to cluster together.

3.1.4. Applied voltage

The applied voltage is a key parameter in achieving a stable cone-jet mode for the obtention of monodispersed nanoparticles. In the present study, with zein concentrations of 2.5% and 5% (w/w) it was not possible to obtain a stable cone-jet mode for voltages other than 14 kV. When the concentration of the polymer solution was increased to 10% (w/w), a stable cone-jet mode was achieved under voltages of both 14 kV (Fig. 5A) and 16 kV (Fig. 5B). Compared to the previous results for 14 kV, the higher voltage (16 kV) did not change the shape of the particles to any considerable degree; this behavior is in agreement with previous works (Hartman et al., 2000; Hong et al., 2008; Tang & Gomez, 1996). However, at 16 kV, small particles formed from satellite droplets were also obtained. Hartman et al. (1999) have reported that the current through the liquid cone increases with the applied voltage, affecting the jet break-up mechanism. The mode in which the electrified jet breaks up depends on the stress ratio at the jet surface, which is given by

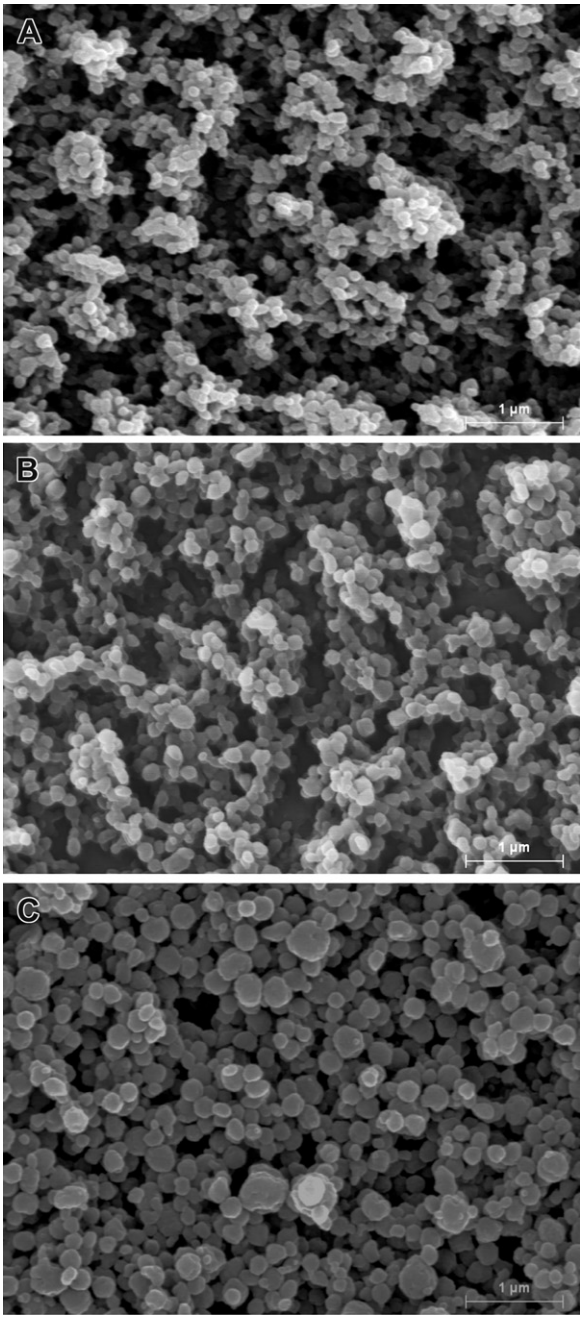

Fig. 4. SEM images showing the effect of flow rate on the size of zein nanoparticles obtained at a constant zein concentration (2.5%), needle-to-tip distance (7 cm) and voltage (14 kV). A: 0.05 mL/h; B: 0.1 mL/h; C: 0.15 mL/h.

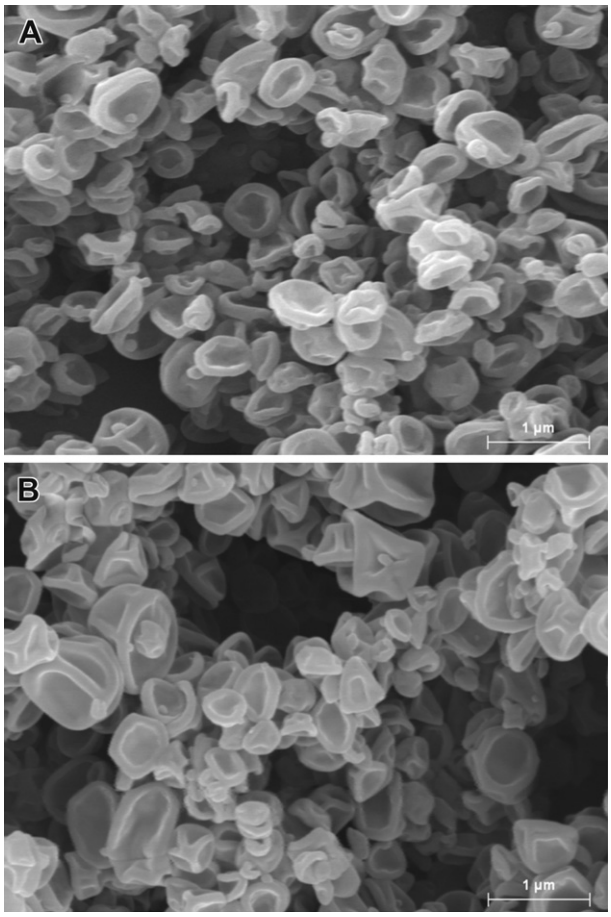

Fig. 5. SEM images showing the effect of applied voltage on the size of zein nanoparticles obtained at a constant zein concentration (10%), needle-to-tip distance (7 cm) and flow rate (0.15 mL/h). A: 14 kV; B: 16 kV.

Table 1
Lightness (L^*), chroma (C^*) and hue angle (h°) of the curcumin-loaded zein nanoparticles (various concentrations), the commercial curcumin and the zein nanoparticles. The total color difference (ΔE) is calculated with respect to the zein nanoparticles.

	L^*	C^*	h°	ΔE
Commercial curcumin	62.1 ± 0.1 a	74.5 ± 0.1 f	62.6 ± 0.03 a	–
1:10 curcumin-loaded zein nanoparticles	65.6 ± 0.8 b	80.5 ± 0.6 g	88.5 ± 0.1 b	35.3 ± 0.4 a
1:20 curcumin-loaded zein nanoparticles	66.5 ± 3.0 b	69.6 ± 2.0 e	91.4 ± 0.3 c	36.5 ± 0.7 a
1:50 curcumin-loaded zein nanoparticles	78.1 ± 4.6 c	59.1 ± 3.4 d	95.9 ± 0.6 d	41.2 ± 1.5 b
1:100 curcumin-loaded zein nanoparticles	82.8 ± 2.1 c	50.6 ± 4.1 c	100.2 ± 2.1 e	53.0 ± 1.8 c
1:500 curcumin-loaded zein nanoparticles	83.1 ± 1.0 c	22.4 ± 1.0 b	102.3 ± 0.5 f	59.8 ± 0.7 d
Zein nanoparticles	83.9 ± 1.1 c	5.1 ± 0.52 a	108.8 ± 0.7 g	–

Different letters in the same column (a, b, c, d, e, f, g) indicate significant differences ($p \leq 0.05$) among samples.

the ratio of the normal electric stress to the surface tension stress. At a low stress ratio value the jet breaks up due to axisymmetric instabilities, also known as varicose instabilities. In this varicose break-up mode, monodisperse droplets are produced and the number of secondary droplets is lower than the number of primary droplets. At high flow rates, the current through the jet of liquid increases, raising the surface charge and the stress ratio. Above a stress ratio threshold value the jet begins to whip and lateral instabilities contribute to the break-up of the jet, resulting in a rise in the number of secondary droplets and satellites, as in the case of the present work when the voltage was set at 16 kV.

3.2. Curcumin-loaded zein nanoparticles

Morphology and encapsulation efficiency (EE)

Based on the previous study discussed above, the processing parameters for obtaining compact spherical nanoparticles with a narrow size distribution were: protein concentration 2.5% (w/w), flow rate 0.15 mL/h, voltage 14 kV, and maintaining a working distance of 7 cm. Curcumin was dissolved into a 2.5% (w/w) ethanolic solution of zein at several concentrations to achieve curcumin:zein weight ratios of 1:500, 1:100, 1:50, 1:20 and 1:10. At all these curcumin concentrations, the curcumin-loaded zein nanoparticles presented a similar morphology and size distribution to those of the unloaded zein nanoparticles obtained from a 2.5% zein solution (data not shown). Consequently, adding curcumin to the zein solution appears not to have affected the electrospray process and thus the formation of the zein nanoparticles, at least at the concentrations assayed in this work. The EE of all the samples was around 85–90%, so a large amount of curcumin was loaded into the nanoparticles. Using the electrospray technique, it is possible to obtain high EE compared to other methods, such as wet or emulsion-based techniques, which involve extracting the particles from an aqueous phase. Other authors have also reported the high encapsulation efficiency achieved by electrospraying, ranging from 80% to 96% (Ding, Lee, & Wang, 2005; Xie, Marijnissen, & Wang, 2006). In other work, it has been encapsulated hydrophilic bovine serum albumin in the hydrophobic polymers PLGA and PCL, concluding that EE greatly depends on the interactions between the polymer, protein, and organic solvent, and that if the interactions are unfavorable the incorporation of surfactants can improve the stability of the system, increasing the EE (Xu & Hanna, 2006). A feasible explanation for the good EE of curcumin in zein nanoparticles could be their good solubility in the solvent and, according to results showed forward, the intimate contact between both components.

3.2.1. Optical properties

The optical properties of the curcumin-loaded zein nanoparticles are shown in Table 1. A trend towards increased lightness can be observed as the curcumin concentration in the nanoparticles decreased, with the maximum lightness value being attained by the plain zein nanoparticles. The hue angle also increased as the curcumin concentration in the nanoparticle decreased. As expected, an evident decrease in the chroma value was obtained when the curcumin concentration in the nanoparticle was reduced. This shows the usefulness of nanoencapsulating natural dyes to achieve a variety of different chroma and hue angle in addition to those of the unprocessed compounds.

3.2.2. Fluorescence microscopy

In previous experiments in which the individual components (curcumin and zein) were investigated separately, it was observed that curcumin emitted intensely in the green region, to a lesser extent in the red one, and was almost imperceptible in the blue region, whereas zein showed no autofluorescence under the experimental conditions employed (Medrano, 2010). Fig. 6 shows the fluorescence microscopy image of the green region of the 1:10 curcumin-loaded zein nanoparticles. The presence of round shapes and apparently compact structures with a narrow size distribution can be observed, together with the green autofluorescence of the curcumin distributed evenly throughout the zein nanoparticle.

3.2.3. Solid state characterization

The X-ray powder diffraction spectra of commercial curcumin, zein nanoparticles and curcumin-loaded zein nanoparticles are shown in Fig. 7. The zein nanoparticles did not display any crystalline peak in the diffractogram but showed one broad amorphous peak. The curcumin diffractogram has the characteristically well-defined sharp, narrow diffraction peaks of a highly crystalline structure. Non-crystalline curcumin peaks were seen when the curcumin was entrapped in the zein nanoparticles; this was observed for all the curcumin:zein ratios tested, revealing the amorphous state of the curcumin in the zein nanostructures. The disruption of the crystalline structure of curcumin is proof of the intimate contact between this compound and the zein protein,

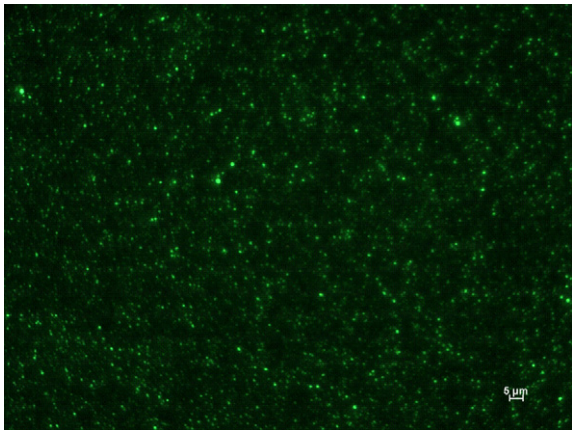

Fig. 6. Fluorescence microscopy image of 1:10 curcumin-loaded zein nanoparticles. The image was taken with the green filter (excitation at 465–495 nm, emission at 515–555 nm).

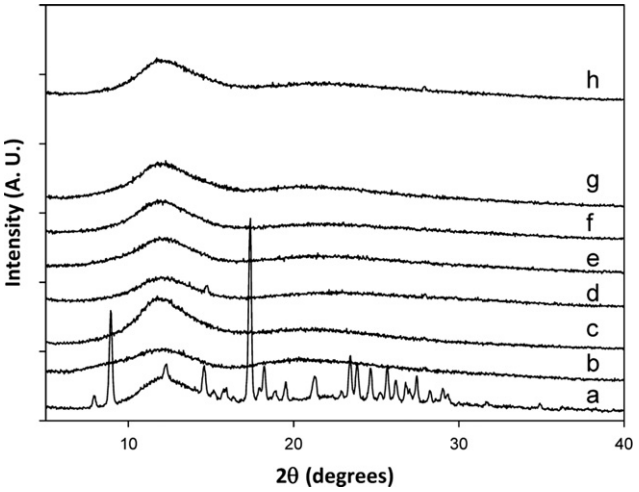

Fig. 7. X-Ray diffraction spectra of zein nanoparticles loaded with different proportions of curcumin. a: commercial curcumin; b: commercial zein; c: 1:10 curcumin-loaded zein nanoparticles; d: 1:20 curcumin-loaded zein nanoparticles; e: 1:50 curcumin-loaded zein nanoparticles; f: 1:100 curcumin-loaded zein nanoparticles; g: 1:500 curcumin-loaded zein nanoparticles. Trace h represents the spectra of the 1:10 curcumin-loaded zein nanoparticles stored for 90 days (43% RH, 23 °C, dark conditions).

which inhibits the curcumin molecules' associating to form crystals (Rawlinson, Williams, Timmins, & Grimsey, 2007).

3.3. Curcumin-loaded zein nanoparticle stability studies

The morphology and size of the zein nanoparticles loaded with curcumin at a weight ratio of 1:10 and stored at 23 °C and 43% relative humidity did not suffer significant changes after three months of storage (Fig. 8). The round shape and compact structure of the nanoparticles remained stable, agglomerates were not observed and the nanoparticles did not shrink but maintained their size. After three months of storage there was no recrystallization of the curcumin in the nanoparticles, which retained its amorphous state (Fig. 7, trace h). No changes were observed in the curcumin content of the nanoparticle (data not shown) or in the physical appearance of the powder after three months of storage in dark conditions.

3.4. Coloring capacity of curcumin-loaded zein nanoparticles in semi-skimmed milk

Fig. 9 and Table 2 respectively show the visual aspect and the color coordinates (lightness, chroma, hue angle, and total color difference) of the milk samples. The addition of commercial curcumin scarcely modified the lightness, chroma and hue angle of the milk, resulting in a total color difference of 4.0 ± 0.1 compared to the aqueous milk without additions. This demonstrates the low solubility of this food coloring in the food matrix employed. On

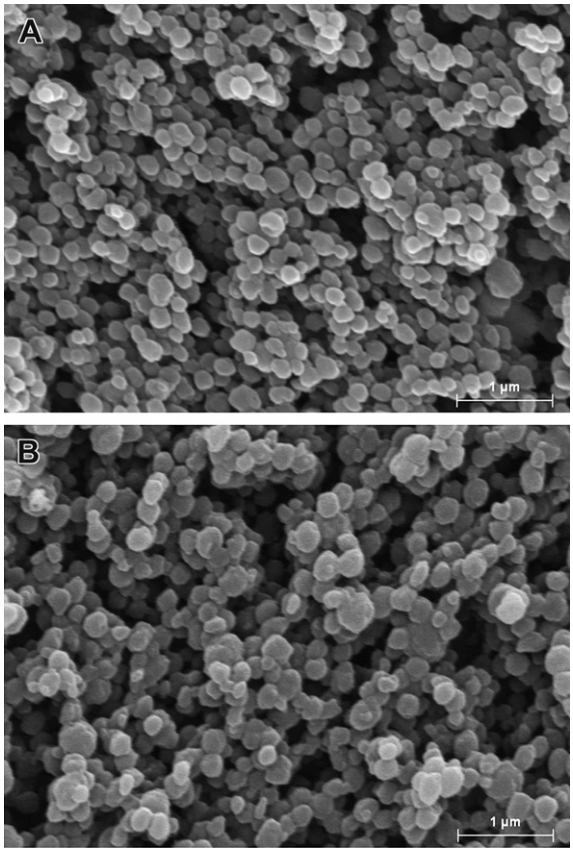

Fig. 8. SEM images showing the effect of storage (43% RH, 23 °C, dark conditions) on the morphology of 1:10 curcumin-loaded zein nanoparticles. A: day 0; B: day 90.

adding the same amount of curcumin (0.1 g/100 mL) incorporated into the zein nanoparticles, the hue angle changed from 110.7° ± 0.1 to 96.6° ± 0.1, the chroma rose from 7.8 ± 0.1 to 61.7 ± 0.1 and the lightness diminished from 87.8 ± 0.1 to 83 ± 0.1 compared to the milk without additions, so the total color difference was 51.3 ± 0.1. The change in milk color as a result of adding the curcumin-loaded zein nanoparticles is also evident in Fig. 9. The addition of a higher amount of curcumin (0.15 g/100 mL) did not produce an increase in chromaticity and the lightness, hue angle and total color difference were scarcely modified, presumably indicating that the color was saturated. When a lower amount of curcumin was added (0.05 g/100 mL) the chromaticity increased to a lower extent than with 0.1 g/100 mL, the hue angle shifted from 96.6 ± 0.1 to 102.5 ± 0.1 and the total color difference was 39.3 ± 0.1. Consequently, this experiment shows that it is possible to obtain milk-based products with different shades and chromaticities by adding different amounts of curcumin-loaded zein nanoparticles.

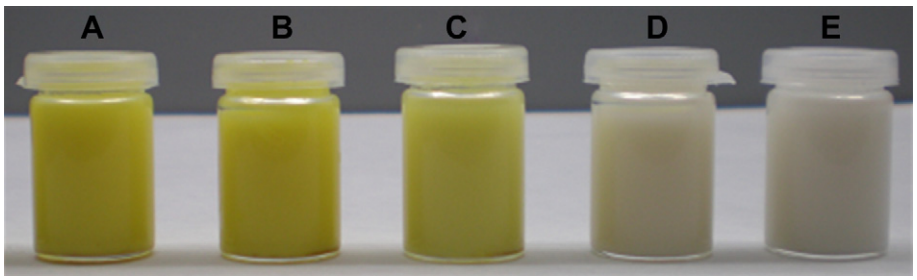

Fig. 9. Capacity of 1:10 curcumin-loaded zein nanoparticles to color semi-skimmed milk. A: 0.15 g of nanoencapsulated curcumin/100 mL milk; B: 0.1 g of nanoencapsulated curcumin/100 mL milk; C: 0.05 g of nanoencapsulated curcumin/100 mL milk; D: 0.1 g commercial curcumin/100 mL milk; E: milk without additions.

Table 2
Lightness (L^*), chroma (C^*), hue angle (h°) and total color difference (ΔE) of the milk containing 1:10 curcumin-loaded zein nanoparticles. The total color difference is calculated with respect to the milk without additions.

	L^*	C^*	h°	ΔE
Milk without additions	87.8 ± 0.1 a	7.8 ± 0.1 a	110.7 ± 0.1 a	–
Commercial curcumin (0.1 g/100 mL milk)	87.6 ± 0.1 a	11.8 ± 0.1 b	108.5 ± 0.1 b	4.0 ± 0.1 a
Curcumin-loaded zein nanoparticles (0.05 g curcumin/100 mL milk)	85.6 ± 0.1 b	47.0 ± 0.1 c	102.5 ± 0.1 c	39.3 ± 0.1 b
Curcumin-loaded zein nanoparticles (0.1 g curcumin/100 mL milk)	83.0 ± 0.1 c	61.7 ± 0.1 d	96.6 ± 0.1 d	51.3 ± 0.1 c
Curcumin-loaded zein nanoparticles (0.15 g curcumin/100 mL milk)	79.4 ± 0.1 d	60.3 ± 0.2 d	95.7 ± 0.1 e	53.5 ± 0.3 c

Different letters in the same column (a, b, c, d, e) indicate significant differences ($p \leq 0.05$) among samples.

4. Conclusions

EHDA has shown itself to be a valuable tool for obtaining nanoparticles of an edible zein biopolymer in several morphologies and sizes depending on the different key parameters controlling the process. Compact spherical nanoparticles were obtained from 2.5% zein solution, fixing the flow rate and voltage at 0.15 mL/h and 14 kV; increasing the polymer concentration to 15% gave rise to particles of greater size and non-spherical morphologies. Small compact nanoparticles could not be achieved for 1% zein solution. The transition from particles to fibers happened between 15% and 20% zein solution. The flow rate affected to the size of the particles whereas high voltages increased the size distribution of the particles. Nanoparticles made from 2.5% zein solution using a flow rate of 0.15 mL/h and a voltage of 14 kV were loaded with several amounts of curcumin comprised between 1:500 and 1:10, achieving in all the cases great encapsulation efficiency. The curcumin mixed intimately with the polymer in a matrix system where the curcumin remained in the amorphous state, unlike commercial curcumin. No changes in the morphology of the nanoparticles or the curcumin content of the nanoparticle during storage (23 °C and 43% RH, in the dark) were observed. The nanoparticles showed good dispersion and coloring capacity in semi-skimmed milk compared to commercial curcumin. Thus, electrospray/electrohydrodynamic atomization technique enables to obtain zein compact nanoparticles charged with curcumin making possible to extend the use of curcumin like a coloring agent in aqueous food products.

Acknowledgments

The authors wish to thank to the Spanish Ministry of Science and Innovation for financial support through projects INGENIO-CONSOLIDER CSD2007-00063 and AGL-2009-08776. Mary Georgina Hardinge provided assistance with the English language text.

References

Ahsan, H., Parveen, N., Khan, N. U., & Hadi, S. M. (1999). Pro-oxidant, anti-oxidant and cleavage activities on DNA of curcumin and its derivatives demethoxycurcumin and bisdemethoxycurcumin. *Chemico-Biological Interactions, 121*(2), 161–175.

Ammon, H. P. T., & Wahl, M. A. (1991). Pharmacology of curcuma-longa. *Planta Medica, 57*(1), 1–7.

Baglole, K. N., Boland, P. G., & Wagner, B. D. (2005). Fluorescence enhancement of curcumin upon inclusion into parent and modified cyclodextrins. *Journal of Photochemistry and Photobiology A-Chemistry, 173*(3), 230–237.

Biswas, T. K., & Mukherjee, B. (2003). Plant medicines of Indian origin for wound healing activity: a review. *International Journal of Lower Extremity Wounds, 2*(1), 25–39.

Chin, S. F., Iyer, K. S., Saunders, M., St Pierre, T. G., Buckley, C., Paskevicius, M., et al. (2009). Encapsulation and sustained release of curcumin using superparamagnetic silica reservoirs. *Chemistry-a European Journal, 15*(23), 5661–5665.

Das, R. K., Kasoju, N., & Bora, U. (2010). Encapsulation of curcumin in alginate-chitosan-pluronic composite nanoparticles for delivery to cancer cells. *Nanomedicine-Nanotechnology Biology and Medicine, 6*(1), 153–160.

Ding, L., Lee, T., & Wang, C. H. (2005). Fabrication of monodispersed taxol-loaded particles using electrohydrodynamic atomization. *Journal of Controlled Release, 102*(2), 395–413.

Dror, Y., Ziv, T., Makarov, V., Wolf, H., Admon, A., & Zussman, E. (2008). Nanofibers made of globular proteins. *Biomacromolecules, 9*(10), 2749–2754.

Hartman, R. P. A., Brunner, D. J., Camelot, D. M. A., Marijnissen, J. C. M., & Scarlett, B. (1999). Electrohydrodynamic atomization in the cone-jet mode physical modeling of the liquid cone and jet. *Journal of Aerosol Science, 30*(7), 823–849.

Hartman, R. P. A., Brunner, D. J., Camelot, D. M. A., Marijnissen, J. C. M., & Scarlett, B. (2000). Jet break-up in electrohydrodynamic atomization in the cone-jet mode. *Journal of Aerosol Science, 31*(1), 65–95.

Hong, Y. L., Li, Y. Y., Yin, Y. Z., Li, D. M., & Zou, G. T. (2008). Electrohydrodynamic atomization of quasi-monodisperse drug-loaded spherical/wrinkled microparticles. *Journal of Aerosol Science, 39*(6), 525–536.

Huang, Q. R., Yu, H. L., & Ru, Q. M. (2010). Bioavailability and delivery of nutraceuticals using nanotechnology. *Journal of Food Science, 75*(1), R50–R57.

Jayaprakasha, G. K., Rao, L. J., & Sakariah, K. K. (2006). Antioxidant activities of curcumin, demethoxycurcumin and bisdemethoxycurcumin. *Food Chemistry, 98*(4), 720–724.

Jayaprakasha, G. K., Rao, L. J. M., & Sakariah, K. K. (2002). Improved HPLC method for the determination of curcumin, demethoxycurcumin, and bisdemethoxycurcumin. *Journal of Agricultural and Food Chemistry, 50*(13), 3668–3672.

Jurenka, J. S. (2009). Anti-inflammatory properties of curcumin, a major constituent of curcuma longa: a review of preclinical and clinical research. *Alternative Medicine Review, 14*(2), 141–153.

Kim, M. K., Choi, G. J., & Lee, H. S. (2003). Fungicidal property of *Curcuma longa* l. Rhizome-derived curcumin against phytopathogenic fungi in a greenhouse. *Journal of Agricultural and Food Chemistry, 51*(6), 1578–1581.

Laemmli, U. K. (1970). Cleavage of structural proteins during assembly of head of bacteriophage-t4. *Nature, 227*(5259), 860–865.

Landry, J., & Guyon, P. (1984). Zein of maize grain .1. Isolation by gel-filtration and characterization of monomeric and dimeric species. *Biochimie, 66*(6), 451–460.

Li, L., Ahmed, B., Mehta, K., & Kurzrock, R. (2007). Liposomal curcumin with and without oxaliplatin: effects on cell growth, apoptosis, and angiogenesis in colorectal cancer. *Molecular Cancer Therapeutics, 6*(4), 1276–1282.

Li, Y., Lim, L., & Kakuda, Y. (2009). Electrospun zein fibers as carriers to stabilize (-)-epigallocatechin gallate. *Journal of Food Science, 74*(3), C233–C240.

Lin, C. C., Lin, H. Y., Chen, H. C., Yu, M. W., & Lee, M. H. (2009). Stability and characterisation of phospholipid-based curcumin-encapsulated microemulsions. *Food Chemistry, 116*(4), 923–928.

Liu, X. M., Sun, Q. S., Wang, H. J., Zhang, L., & Wang, J. Y. (2005). Microspheres of corn protein, zein, for an ivermectin drug delivery system. *Biomaterials, 26*(1), 109–115.

Medrano, N. (2010). *Nanoencapsulación de compuestos bioactivos de interés alimentario en biopolímeros comestibles mediante atomización electrohidrodinámica.* Valencia, Spain: Universidad Politécnica de Valencia.

Meng, F. Z., Jiang, Y., Sun, Z. H., Yin, Y. Z., & Li, Y. Y. (2009). Electrohydrodynamic liquid atomization of biodegradable polymer microparticles: effect of electrohydrodynamic liquid atomization variables on microparticles. *Journal of Applied Polymer Science, 113*(1), 526–534.

Mukerjee, A., & Vishwanatha, J. K. (2009). Formulation, characterization and evaluation of curcumin-loaded PLGA nanospheres for cancer therapy. *Anticancer Research, 29*(10), 3867–3875.

Onal, U., & Langdon, C. (2005). Performance of zein-bound particles for delivery of riboflavin to early fish larvae. *Aquaculture Nutrition, 11*(5), 351–358.

Parris, N., Cooke, P. H., & Hicks, K. B. (2005). Encapsulation of essential oils in zein nanospherical particles. *Journal of Agricultural and Food Chemistry, 53*(12), 4788–4792.

Patel, A., Hu, Y. C., Tiwari, J. K., & Velikov, K. P. (2010). Synthesis and characterisation of zein-curcumin colloidal particles. *Soft Matter, 6*(24), 6192–6199.

Prajakta, D., Ratnesh, J., Chandan, K., Suresh, S., Grace, S., Meera, V., et al. (2009). Curcumin loaded ph-sensitive nanoparticles for the treatment of colon cancer. *Journal of Biomedical Nanotechnology, 5*(5), 445–455.

Raula, J., Eerikainen, H., & Kauppinen, E. I. (2004). Influence of the solvent composition on the aerosol synthesis of pharmaceutical polymer nanoparticles. *International Journal of Pharmaceutics, 284*(1–2), 13–21.

Rawlinson, C. F., Williams, A. C., Timmins, P., & Grimsey, I. (2007). Polymer-mediated disruption of drug crystallinity. *International Journal of Pharmaceutics, 336*(1), 42–48.

Shaikh, J., Ankola, D. D., Beniwal, V., Singh, D., & Kumar, M. (2009). Nanoparticle encapsulation improves oral bioavailability of curcumin by at least 9-fold when compared to curcumin administered with piperine as absorption enhancer. *European Journal of Pharmaceutical Sciences, 37*(3–4), 223–230.

Shukla, R., & Cheryan, M. (2001). Zein: the industrial protein from corn. *Industrial Crops and Products, 13*(3), 171–192.

Sreejayan, & Rao, M. N. A. (1997). Nitric oxide scavenging by curcuminoids. *Journal of Pharmacy and Pharmacology, 49*(1), 105–107.

Tang, K. Q., & Gomez, A. (1996). Monodisperse electrosprays of low electric conductivity liquids in the cone-jet mode. *Journal of Colloid and Interface Science, 184*(2), 500–511.

Tonnesen, H. H. (2002). Solubility, chemical and photochemical stability of curcumin in surfactant solutions – studies of curcumin and curcuminolds, xxviii. *Pharmazie, 57*(12), 820–824.

Villegas, I., Sanchez-Fidalgo, S., & de la Lastra, C. A. (2008). New mechanisms and therapeutic potential of curcumin for colorectal cancer. *Molecular Nutrition & Food Research, 52*(9), 1040–1061.

Wang, Y., Lu, Z. X., Lv, F. X., & Bie, X. M. (2009). Study on microencapsulation of curcumin pigments by spray drying. *European Food Research and Technology, 229*(3), 391–396.

Wang, Y., Lu, Z. X., Wu, H., & Lv, F. X. (2009). Study on the antibiotic activity of microcapsule curcumin against foodborne pathogens. *International Journal of Food Microbiology, 136*(1), 71–74.

Woerdeman, D. L., Ye, P., Shenoy, S., Parnas, R. S., Wnek, G. E., & Trofimova, O. (2005). Electrospun fibers from wheat protein: investigation of the interplay between molecular structure and the fluid dynamics of the electrospinning process. *Biomacromolecules, 6*(2), 707–712.

Wu, Y. Q., MacKay, J. A., McDaniel, J. R., Chilkoti, A., & Clark, R. L. (2009). Fabrication of elastin-like polypeptide nanoparticles for drug delivery by electrospraying. *Biomacromolecules, 10*(1), 19–24.

Xie, J. W., Lim, L. K., Phua, Y. Y., Hua, J. S., & Wang, C. H. (2006). Electrohydrodynamic atomization for biodegradable polymeric particle production. *Journal of Colloid and Interface Science, 302*(1), 103–112.

Xie, J. W., Marijnissen, J. C. M., & Wang, C. H. (2006). Microparticles developed by electrohydrodynamic atomization for the local delivery of anticancer drug to treat c6 glioma in vitro. *Biomaterials, 27*(17), 3321–3332.

Xu, Y. X., & Hanna, M. A. (2006). Electrospray encapsulation of water-soluble protein with polylactide – effects of formulations on morphology, encapsulation efficiency and release profile of particles. *International Journal of Pharmaceutics, 320*(1–2), 30–36.

Yoysungnoen, P., Wirachwong, P., Changtam, C., Suksamram, A., & Patumraj, S. (2008). Anti-cancer and anti-angiogenic effects of curcumin and tetrahydrocurcumin on implanted hepatocellular carcinoma in nude mice. *World Journal of Gastroenterology, 14*(13), 2003–2009.

Yu, H. L., & Huang, Q. R. (2010). Enhanced in vitro anti-cancer activity of curcumin encapsulated in hydrophobically modified starch. *Food Chemistry, 119*(2), 669–674.

Zhong, Q. X., & Jin, M. F. (2009). Nanoscalar structures of spray-dried zein microcapsules and in vitro release kinetics of the encapsulated lysozyme as affected by formulations. *Journal of Agricultural and Food Chemistry, 57*(9), 3886–3894.

Zhong, Q. X., Jin, M. F., Davidson, P. M., & Zivanovic, S. (2009). Sustained release of lysozyme from zein microcapsules produced by a supercritical anti-solvent process. *Food Chemistry, 115*(2), 697–700.